

# CFD ANALYSIS OF THREE-DIMENSIONAL FLOWS IN A LOW REYNOLDS NUMBER MICROTURBINE

Mohamed Omri and Luc G. Fréchette \*

Université de Sherbrooke – Département de génie mécanique  
2500 boul. Université, Sherbrooke, Québec J1K 2R1, Canada

\*Presenting Author: Luc.Frechette@USherbrooke.ca

## Abstract:

In this work, three dimensional numerical studies of the aerodynamics in laminar subsonic cascades at relatively low Reynolds numbers ( $Re < 2500$ ) are presented. The stator and rotor blade designs are those for a MEMS-based Rankine microturbine power-plant-on-a-chip. Blade passage calculations in 2D and 3D were done for different Reynolds numbers and four incidences ( $0^\circ$ ,  $5^\circ$ ,  $10^\circ$  and  $15^\circ$ ) to determine the flow patterns and losses. The 3D stage (without tip clearance) indicates the presence of boundary layers and the presence of two identical vortices due to the interaction between flow curvature and boundary layers. Two dimensional calculations characterize well the flow at the mid-height plane, but are not sufficient for loss predictions due to the omission of these flow structures. The 2D and 3D total losses, increase dramatically for  $Re < 500$ . This suggests an operating Reynolds number greater than 1000 to maintain acceptable efficiency, which is similar to the 2D studies. The losses also increased monotonically with increasing incidence and the 2D assumption can be used to estimate losses but with a correction for 3D effects.

**Keywords:** CFD, Microturbine, vortices, losses

## INTRODUCTION

The design objective of Micro Electro Mechanical Systems (MEMS) based on microturbomachinery is to create power sources on a small scale ( $\text{cm}^3$ ) and with high power density ( $1\text{-}100 \text{ W/cm}^3$ ) [2-5]. The development of micro heat engines requires multi-disciplinary knowledge and requires the comprehension of fluid dynamics and heat transfer through MEMS.

Computational fluid dynamic (CFD) calculations find their rightful place since it is difficult and even impossible to give a fine experimental description of the flow within those small devices. Moreover, limited experimental data is available [4, 6, and 8]. Recently, Beauchesne-Martel & Fréchette [1] gave a complete analysis of the aerothermodynamics of subsonic laminar cascades and design tools for microturbines, based on 2D CFD calculations. This work aims to provide a description of the structure of subsonic laminar cascades (especially in 3D) but also a critical comparison between 2D and 3D calculations.

In this work, we present a detailed description of the 3D flow fields at relatively low Reynolds numbers ( $Re < 2500$ ). The structure and evolution of the flow, along with induced losses are detailed. Special importance is given to the effect of Reynolds number and incidence on the flow structure and losses. So, four incidences (here after referred to as  $\alpha$ )  $0^\circ$ ,  $5^\circ$ ,  $10^\circ$  and  $15^\circ$  are considered.

Section 2 outlines the description and modelling of the problem. The most important results and discussions are presented in section 3.

## 2. DESCRIPTION AND MODELLING OF THE PROBLEM

The device considered here is currently under development [7]. It consists of a 4-mm diameter rotor with a single turbine stage, as illustrated in figure 1.

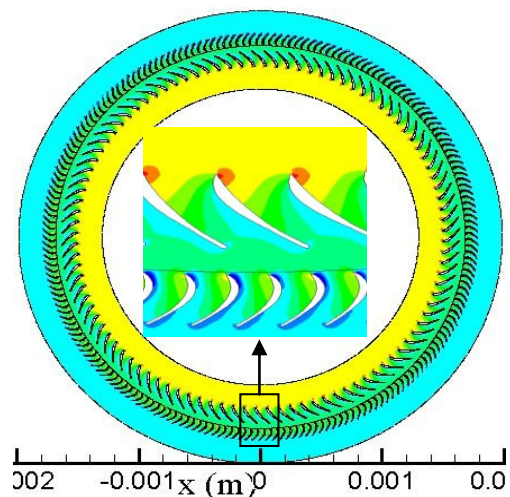


Fig. 1: 2D static pressure contours of the microturbine

Naturally, it is not judicious to consider the whole 3D geometry of the microturbine, since its volute is symmetrical and would require expensive computation time. Thus, only a cascade is sufficient to give an adequate description of the flow and losses within this turbine. Figure 2 gives all details about the geometry and also surfaces where losses are calculated and positions where the velocity profiles will be plotted.

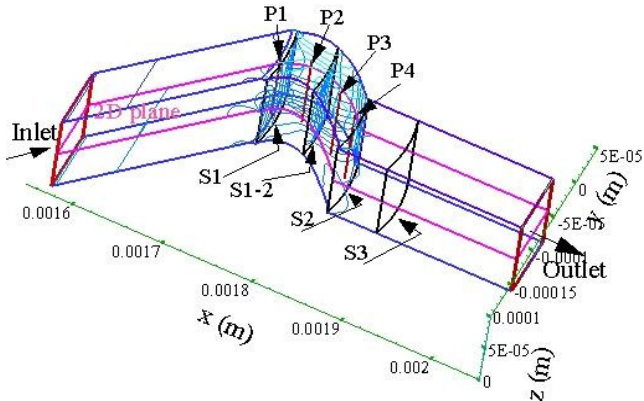


Fig. 2: Sketch of the cascade computational domain, showing the relevant planes and static pressure contours.

The fluid is water vapour, considered as a compressible ideal gas. A stationary adiabatic calculations is performed at different incidences ( $\alpha = 0^\circ, 5^\circ, 10^\circ$  and  $15^\circ$ ), varying the inlet total pressure and the scale of the cascade to vary the inlet Reynolds number (based on the chord length) from 40 to 2500, while maintaining mach number in the range  $[0.3..0.5]$ . The nominal blade dimensions are 109 microns chord and 100 microns height. Inlet temperature is 600 K. Losses are calculated by taking averaged properties at the cascade's inlet (S1) and outlet (S2), and downstream (S3) of the cascade (Fig. 2).

The coupled partial differential equations describing the flow field are discretized with the finite volume method, using a commercial solver (Fluent Inc.). Second order upwind discretization is used. The rectangular staggered grid is non-uniform in both directions: it is finer near the walls where gradients are more important. Convergence is declared when the cumulative residuals for all conservation equations are less than at least  $10^{-8}$ .

### 3. RESULTS AND DISCUSSION

#### 2D vs 3D

Considering flow at the mid-height plane the pressure contours from the 2D calculations are similar to those from the 3D calculations (Fig. 3). The 2D assumption would therefore appear to be acceptable to characterise a microturbine. Evidently, we can not see development of 3D flow structures in the 2D case, as will be discussed later.

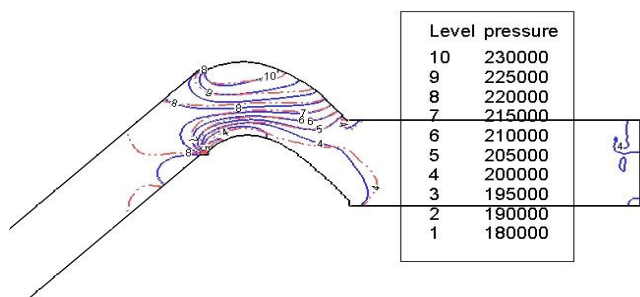


Fig. 3: Static pressure contours in the case of incidence zero at  $Re=840$  (2D versus 3D)

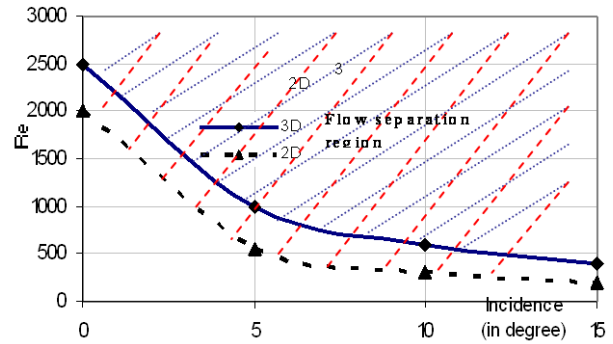


Fig. 4: Critical Reynolds number versus incidence

Another important point is flow separation, which is declared at lower Reynolds number in the 2D case, as indicated in figure 4. This figure, indicating the Reynolds number at which separation occurs (for 2D and 3D calculations) versus the flow incidence angle, shows that the two trends are similar with almost a constant offset, except at high incidence ( $\alpha > 10^\circ$ ).

#### 3D flow structures

The 3D effects are illustrated in figure 5, showing the iso-surfaces of static pressure with stream traces in order to visualise the vortices. The presence of horizontal boundary layers (top and bottom) generates secondary flows, and it forms double vortices in the channel between blades. Since there is no tip clearance in this case (but also at low tip clearances), the two vortices are symmetrical, identical and positioned near the extrados (suction surfaces).

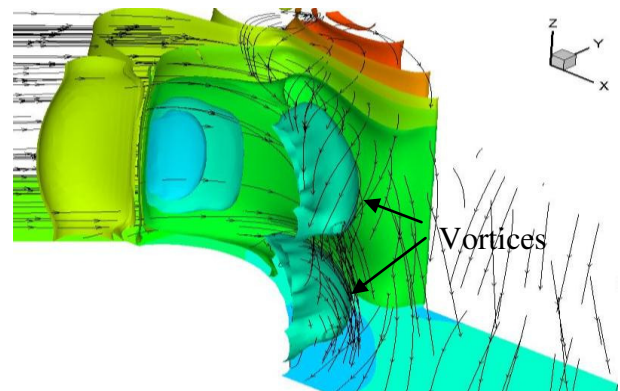


Fig. 5: Iso-surfaces of static pressure with stream traces (3D case without tip clearance).

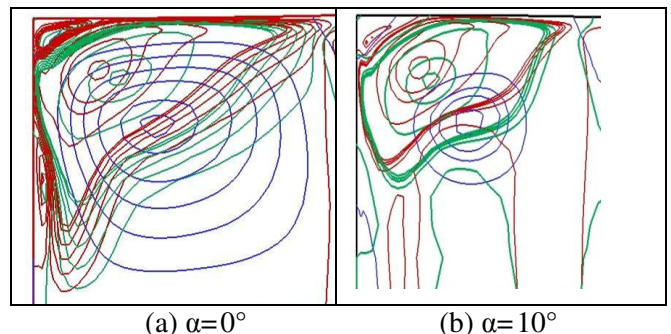


Fig. 6: Helicity contours for three Reynolds numbers:  $Re=140$  (blue),  $Re=1160$  (green) and  $Re=2400$  (red).

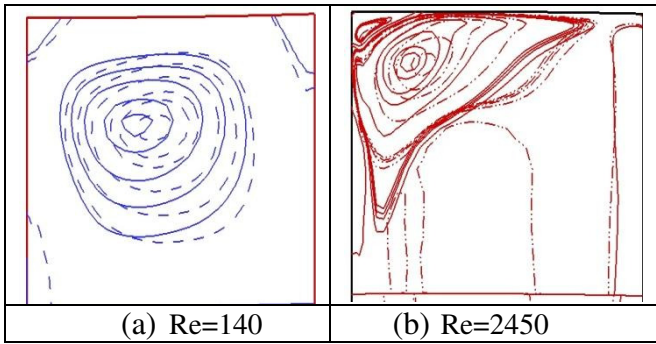


Fig. 7: Helicity contours for  $\alpha = 0^\circ$  (solid) and  $\alpha = 10^\circ$  (dashed)

The vortex trajectories depend on the Reynolds number and also on the flow incidence angle; it is closer to the extrados for highest Reynolds number and lowest incidence angles. As an example, we present in figure 6 a comparison at three different Reynolds numbers ( $Re=140\pm 10$ ,  $1130\pm 30$  and  $2450\pm 60$ ) for  $\alpha=0^\circ$  and  $\alpha=10^\circ$ , taken in the section (S1-2) (figure 2). We see clearly the influence of Reynolds number i.e. by increasing the Reynolds number; the vortices become closer to the extrados (corner). Helicity contours at high Reynolds numbers also indicate the complexity of the flow in the rest of the blade passage. To better highlight the incidence effect, figure 7 overlays the helicity contours for  $\alpha=0^\circ$  and  $\alpha=10^\circ$  at two Reynolds numbers ( $140\pm 10$  and  $2450\pm 60$ ). As shown, the vortices are closer to the extrados at lower incidence.

### Velocity profiles

Figure 8 shows the radial velocity across the blade passage (y-direction) at mid-height of section (1-2) for different incidences and  $Re=1100\pm 20$ . The velocity profiles are qualitatively comparable with a significant different difference between the 2D and 3D cases: the magnitude of the radial velocity is more important in the 3D case with a passage section narrowed along the y direction. Another important point is that the negative values of this velocity indicate the presence of flow separation. The profiles in blue (dashed vs solid) are different, since unlike the 3D case, there is a separation in the 2D case, as also indicated in figure 4. For design, it is useful to decompose the passage into a 2D core-flow region plus hub and tip regions. To evaluate the extent of the core flow region, figure 9 shows the radial velocity along the span (z-direction) at different positions in the meridian plane between blades. From  $Re\approx 1200$  to  $2200$ , the velocity conserves its profile at each position. When changing the incidence flow angle however, the velocity profile is totally different principally in the positions P3 and P4. The flow is highly complex in this region. For  $\alpha = 0^\circ$ , the 2d assumption covers about 70% ( $0.15 < z/z_{max} < 0.85$ ) of the whole inter-blade volume; this is not truth when  $\alpha=15^\circ$ . At high incidences, the flow becomes complex near the outlet blades region

excluding the usefulness of the 2D core-flow assumption.

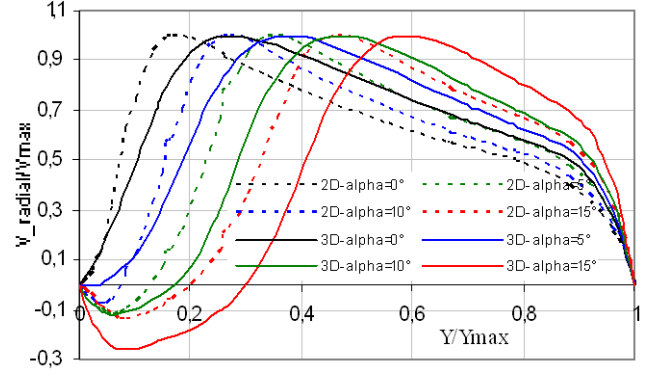


Fig. 8: Normalized radial velocity profiles across the blade passage. Two dimensional versus 3D cases at  $\alpha=0^\circ, 5^\circ, 10^\circ$  and  $15^\circ$  ( $Re\approx 1100$ )

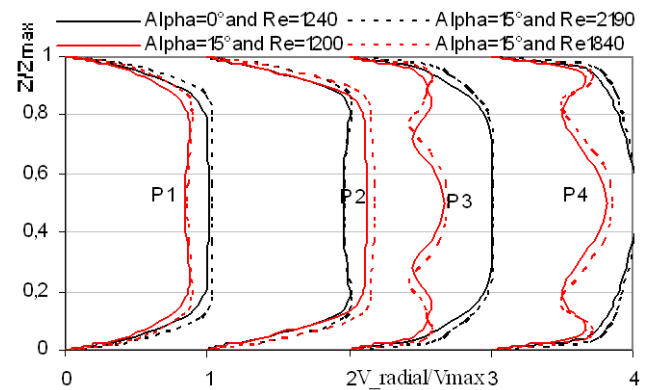


Fig. 9: Radial velocity at different positions (P1,P2,P3 and P4) at two incidences and two Reynolds numbers.

### 2D vs 3D losses

Certainly understanding the flow structure in the microturbine is essential, but practical quantities such as losses are necessary for device design. This section presents the 3D losses and compares them to losses for 2D calculations. The total losses are calculated as the sum of profile losses and mixing losses (see [8]); in the 3D case the average of each quantity " $\Phi$ " in a considered section is determined as:  $(\int \rho V_x \Phi dS) / \int \rho V_x dS$ . Figure 10 indicates the total losses (2D and 3D) versus the Reynolds number at four different incidences. The total losses, increase dramatically for  $Re < 500$ .

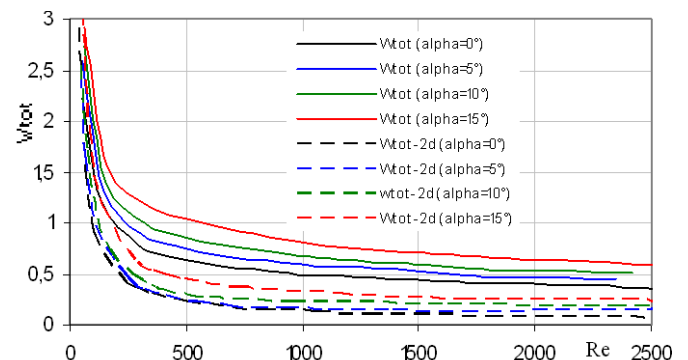


Fig. 10: Total losses at different incidences (2D versus 3D)

This suggests that the operating range for sub-millimeter blade chords should be in the hundreds of m/s to maintain acceptable efficiency, which is similar to conclusions from 2D calculations. Design approaches based on 2D calculations for loss predictions, clearly necessitates a correction since it underestimates total losses. The 3D losses also increased monotonically by varying the incidence from  $0^\circ$  to  $15^\circ$ ; this tendency is less clear in the 2D case.

The total losses, which are calculated as the sum of profile losses and mixing losses seem conditioned principally by profile losses since mixing losses are negligible as indicated in the figure 11. For  $Re$  greater than 1000, the profile losses are the double of mixing losses except at high incidence ( $15^\circ$ ); then it is possible to consider at this range only the profile losses to characterise the microturbine.

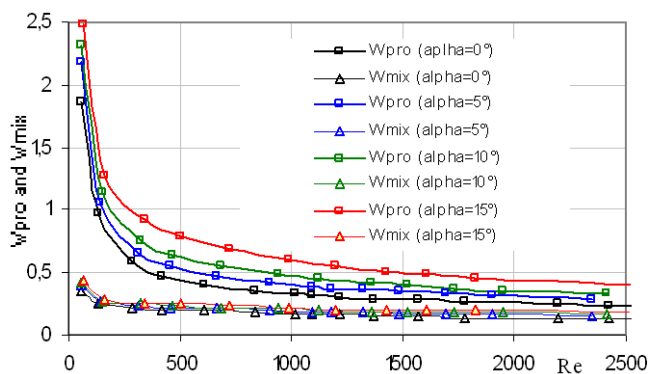


Fig. 11: Profile losses compared to mixing losses in 3D case at  $\alpha=0^\circ, 5^\circ, 10^\circ$  and  $15^\circ$ .

### Other 3D effects

Calculations were done by considering a passage with a realistic inlet to investigate its impact on the flow uniformity. As shown in Fig. 12, a quiescent zone near the axis is formed and a recirculation zone appears after the 90 deg turn. The stator blades are in general positioned within this recirculation zone, which leads to non-uniform stator inlet profiles. The stator tends to eliminate the recirculation since they behave like a convergent, providing more uniform flow to the rotor.

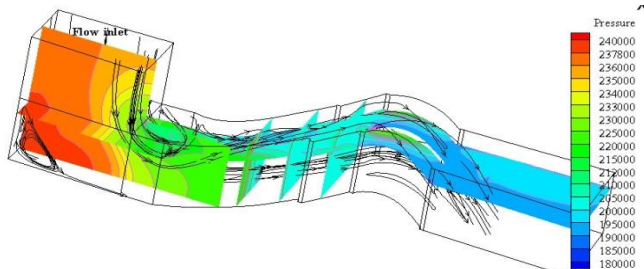


Fig. 12: Complete 3D stage (contours of static pressure).

## CONCLUSIONS

This paper presented a numerical analysis of subsonic laminar flow through a cascade for

microturbomachinery applications operating at low  $Re$ . Numerical calculations using Fluent were done with 2D and 3D geometries at for  $40 \leq Re \leq 2500$ . The 2D assumption can be used to characterise a microturbine, taking into account that it under estimates losses and also indicates premature flow separation. 3D calculations are more representative of the flow structure and losses within the device. They indicate the presence of two symmetrical positioned vortices near the blade extrados. The trajectory of these vortices depends on the Reynolds number and incidence. The losses also increased monotonically with increasing incidence and the 2D assumption can be used to estimate losses but with a correction factor. It is recommended to operate microturbomachinery at Reynolds numbers greater than 1000 to maintain acceptable efficiency. In this range, total losses can be deduced from profile losses only since mixing losses are relatively constant and less important.

## REFERENCES

- [1] Beauchesne-Martel P. and Fréchette, L. G. Numerical Analysis of Sub-Millimeter-Scale Microturbomachinery Aerothermodynamics. In Proc. ASME IMECE 2008-68190, Boston, MA, Oct. 31 – Nov. 6, 2008.
- [2] EPSTEIN, A. H and Senturia, S. D. Macro power from micro machinery. Science, vol. 276, p. 1211, 1997.
- [3] EPSTEIN, A. H., ET AL. Micro-Heat Engines, Gas Turbines, and Rocket Engines - the MIT Microengine Project, AIAA, Snowmass Village, V.97, #28th AIAA Fluid Dynamics Conference, p. 1773, 1997.
- [4] Fréchette, L., Lee, C. S. Arslan, and Y. -C. Liu, Design of a Microfabricated Rankine Cycle Steam Turbine for Power Generation, in Proc. of the ASME IMECE 2003-42082, Washington, DC, 2003.
- [5] Lang, J. J. Multi-Wafer Rotating MEMS Machines: Turbines, Generators, and Engines, New York: Springer, 2009.
- [6] LEE, C., Arslan, S. and FRECHETTE, L. G. Design Principles and Measured Performance of Multistage Radial Flow Microturbomachinery at Low  $Re$  Numbers. J. F. Eng. 130, 111103, 2008.
- [7] Liamini, M., Shahriar, H., Vengallatore, S. and Fréchette, L. Thermal and structural considerations in the design of a Rankine vapour microturbine,” Proc. PowerMEMS 2008, Sendai, Japan, November 9-12, pp. 109-112, 2008.
- [8] MEHRA, A. Computational Investigation and Design of Low Reynolds Number Micro-Turbomachinery, S.M. Thesis, Massachusetts Institute of Technology, Cambridge, MA, p. 132, 1997.